Experimental validation of numerical model for evaluation of local heat transfer coefficient in coiled tubes

IOP Conf. Series: Journal of Physics: Conf. Series **1224** (2019) 012012 doi:10.1088/1742-6596/1224/1/012012

Experimental validation of numerical model for evaluation of local heat transfer coefficient in coiled tubes

P Vocale[a], M Abbenante[b], F. Bozzoli[a,b], S Rainieri[a,b], G Pagliarini[a,b]
[a]Department of Engineering and Architecture, University of Parma, Parco Area delle Scienze 181/A, 43124 Parma – Italy
[b]CIDEA Interdepartmental Centre, University of Parma, Parco Area delle Scienze 181/A, 43124 Parma – Italy

E-mail: pamela.vocale@unipr.it

Abstract. The efficiency of the enhanced heat transfer equipment was widely investigated in literature by adopting both experimental and numerical approaches. Obviously, the numerical tools allow improving the knowledge of the fundamental heat transfer mechanisms in curved geometries, since they enable to evaluate punctually the velocity and temperature distributions. On the other hand, it has to be pointed out that the numerical results can be considered reliable only if they are validated throughout the comparison with either analytical results or experimental data. The validation of numerical models is usually carried out by considering average heat transfer performances, therefore this approach does not guarantee that these models enable to evaluate the local heat transfer phenomena with the same accuracy. In the present paper a promising numerical tool for evaluating local convective heat transfer in coiled-tubes, within the laminar regime, is presented. The Navier-Stokes and energy equations are solved by means of the open-source CFD software OpenFOAM®, with second-order accurate finite-volume schemes, within the framework of the SIMPLE algorithm. The robustness of the numerical model is assessed by comparing the numerical outcomes to the local experimental data available in literature.

1. Introduction

The performances of passive heat transfer enhancement techniques were widely investigated in literature by adopting both experimental and numerical approaches. Although the numerical methodologies enable to evaluate what happens within the fluid, thus providing a better understanding of the heat transfer enhancement mechanism, it has to be pointed out that numerical models can be considered relevant if they are validated against either analytical results or experimental evidences.
One of the simplest passive heat transfer enhancement technique, commonly used in several industrial applications, is based on the use of coiled tube because, for given operating conditions, in this kind of devices heat transfer rate is more effective than in straight pipes [1].
Due to the influence of the wall conformation on the thermal performance of heat transfer equipment, many research group developed numerical models to investigate laminar heat transfer in curved tubes [2-11]. In particular, Mori and Nakayama [2,3] investigated the effect of the secondary flow due to the curvature on the heat transfer coefficient both analytically and experimentally considering different thermal boundary conditions, namely constant wall heat flux and uniform wall temperature. By means

of first and second order solutions of the boundary-layer approximation equations, they proposed simple practical correlations to evaluate the Nusselt number as a function of the main parameters that affect the fluid behaviour.
The limits of the boundary-layer approximation approach was highlighted by Mitsunobu and Cheng [4] who analysed fully developed laminar forced convection in curved pipes and presented a finite-difference solution obtained by means of a combination of line iterative method and boundary vorticity method. Their numerical outcomes showed the effect of Prandtl number on the convective heat transfer coefficient.
The influence of Dean number on the fluid flow behaviour was investigated by Patankar et al. [5] who presented a numerical analysis of local convective heat transfer coefficient for Prandtl number equal to 0.7.
Kozo and Aoyama [6] theoretically and numerically investigated the effect of the secondary flow on heat transfer in uniformly heated helically coiled tube, by accounting for both the centrifugal and buoyancy forces. By analysing several operating conditions, they proposed an approximate correlation that enables to evaluate the Nusselt number as a function of main parameters that influence the fluid behaviour. The effect of buoyancy in helical pipe was also studied by Zheng et al. [7] who accounted for the influence of thermal radiation in a participating medium, as well.
Yang et al. [8, 9] presented numerical investigations on the fully developed laminar convective heat transfer in a helicoidal pipe, with particular attention to the effects of Dean and Prandtl numbers and of torsion on the local convective heat-transfer coefficient. In particular, as concern the effect of torsion induced by the coil pitch [9], the authors reported the Nusselt number distribution for different values of the coil pitch, and they showed that, due to torsion, the local heat-transfer coefficient, compared to the case of an ideal torus, is increased on half of the tube wall while it is decreased on the other half.
Recently, Ko [10] numerically studied the entropy generation rate in helical pipes, by considering water as working fluid and several values of wall heat flux. For each operating condition analysed, his numerical results suggested the optimal Reynolds number to minimize the entropy generation.
However, it has to be pointed out that many of the works available in literature are focused only on the numerical analysis of the average performance of the coiled tubes. Since the flow velocity and temperature fields in coiled ducts are strongly asymmetrical over the cross-section of the tube, local effects have to be accounted for when a numerical model has to be developed. Moreover, local behaviour can affect the performances of many industrial processes. For instance, in food pasteurisation, the irregular temperature field induced by the wall curvature could reduce the effect of the bacteria heat-killing or could locally overheat the product. To the Authors' best knowledge, only few papers present numerical results in terms of local Nusselt number.
Furthermore, it has to be pointed out that the numerical models that were developed to analyse the local convective heat transfer coefficient, were validated only in terms of average performances. Therefore, it is not guaranteed that the so validated models enable to properly evaluate local heat transfer phenomena.
More recently, Bozzoli et al. [11] presented a preliminary numerical analysis of local convective heat transfer in coiled tubes within laminar flow regime. The adopted model was validated through the comparison of the numerical results with the experimental data in terms of convective heat flux distribution along the boundary of the duct. The comparison highlighted that the adopted numerical model did not allow to capture correctly the local heat transfer phenomena.
Therefore, the present work aims to extend the numerical analysis proposed in [11] by adopting a different numerical model that enables to accurately investigate the local heat transfer phenomena in helically coiled tubes for a fully developed laminar flow. To account for the local interaction between the solid walls and the fluid, the analysis is carried out by considering the conjugate heat transfer problem. The Navier-Stokes and energy equations are solved by using the open-source CFD software OpenFOAM®,
The validation of the here presented numerical model is carried out by comparing the numerical results with the experimental data in terms of local convective heat transfer coefficient.

2. Experimental data

The experimental data used to validate the numerical results were obtained by Bozzoli et al. [11,12] who evaluated the convective heat flux and heat transfer coefficient distributions along the boundary of a helically coiled tube. For sake of clarity it's important to recall here the main operating conditions of the experiments carried out in [12]. The tube was characterized by eight coils following a helical profile along the tube's axis, as shown in Figure 1. The duct was characterized by an internal diameter, a helix diameter and a pitch, 14 mm, 310 mm and 200 mm, respectively (the curvature ratio was about 22.14) while the wall thickness was 1 mm.

Ethylene glycol was used as working fluid while the Reynolds number was varied between 135 and 1006. The fluid was heated by Joule dissipation in the tube wall; indeed the inlet and outlet coiled test sections were equipped with stainless-steel fin electrodes and connected to a power supply, as shown in Figure 1.

The test section was located approximately 9 m downstream of the inlet section, in the region where the laminar boundary layers reached the asymptotic profiles. Therefore, the results obtained for that particular section were representative of the fully developed region.

To minimize the heat exchange with the environment, the heated section was insulated by using neoprene, as shown in Figure 1; on the other hand, a small portion of the external tube wall, near to the outlet section, was uninsulated to make it accessible to an infrared imaging camera. A thin film of opaque paint characterized by uniform and known emissivity coated this portion.

Figure 1. Sketch of test rig used for assessing the performance of the helically coiled tube.

The temperature distribution maps on the external surface of the wall were acquired by using a FLIR SC7000 infrared camera, while the inlet and the outlet fluid bulk temperatures were measured with type-T thermocouples. The acquired temperature distributions were employed as input data of the Inverse Heat Conduction Problem (IHCP) in the wall under a solution approach based on Tikhonov regularization method.

3. Numerical model

The local performance of helically coiled tube was numerically investigated by solving the conjugate heat transfer problem, as shown in Figure 2.

The tube under investigation had the same geometrical and physical properties of the duct tested in [11,12] and described in the previous section.

A Cartesian coordinate system x, y, z was introduced, whose origin was located as shown in Figure 2.

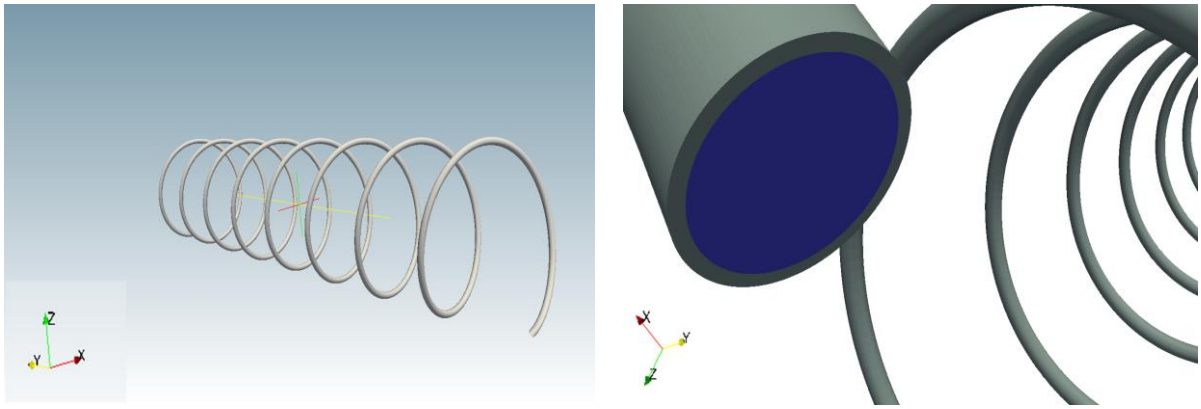

(a) (b)

Figure 2. Geometry under investigation. Sketch of the whole geometric domain (a); zoom on fluid and wall regions, in blue and in grey, respectively (b).

By considering a Newtonian fluid with constant physical properties and by assuming that the flow is laminar and steady-state, the governing equations in Cartesian coordinates are as follows:

$$\frac{\partial u}{\partial x}+\frac{\partial v}{\partial y}+\frac{\partial w}{\partial z}=0 \tag{1}$$

$$\rho\left(u\frac{\partial u}{\partial x}+v\frac{\partial u}{\partial y}+w\frac{\partial u}{\partial z}\right)=-\frac{\partial p}{\partial x}+\mu\left(\frac{\partial^2 u}{\partial x^2}+\frac{\partial^2 u}{\partial y^2}+\frac{\partial^2 u}{\partial z^2}\right)$$

$$\rho\left(u\frac{\partial v}{\partial x}+v\frac{\partial v}{\partial y}+w\frac{\partial v}{\partial z}\right)=-\frac{\partial p}{\partial y}+\mu\left(\frac{\partial^2 v}{\partial x^2}+\frac{\partial^2 v}{\partial y^2}+\frac{\partial^2 v}{\partial z^2}\right) \tag{2}$$

$$\rho\left(u\frac{\partial w}{\partial x}+v\frac{\partial w}{\partial y}+w\frac{\partial w}{\partial z}\right)=-\frac{\partial p}{\partial z}+\mu\left(\frac{\partial^2 w}{\partial x^2}+\frac{\partial^2 w}{\partial y^2}+\frac{\partial^2 w}{\partial z^2}\right)$$

$$\rho\left(u\frac{\partial i}{\partial x}+v\frac{\partial i}{\partial y}+w\frac{\partial i}{\partial z}\right)=\lambda_f\left(\frac{\partial^2 T}{\partial x^2}+\frac{\partial^2 T}{\partial y^2}+\frac{\partial^2 T}{\partial z^2}\right) \tag{3}$$

where u, v and w are the components of the velocity field, ρ, μ, and λ_f are the fluid density, dynamic viscosity and thermal conductivity, respectively, p is the pressure, i the fluid specific enthalpy and T the fluid temperature.
In the solid region, the energy conservation equation reads as follows:

$$\lambda_s\left(\frac{\partial^2 T}{\partial x^2}+\frac{\partial^2 T}{\partial y^2}+\frac{\partial^2 T}{\partial z^2}\right)+q_g=0 \tag{4}$$

being T the temperature of the solid domain, q_g the heat generated by Joule effect in the wall and λ_s the thermal conductivity of the wall.
The governing equations in the fluid region were solved by considering the following boundary conditions at x=0:

$$u=W, \qquad v=0, \qquad w=0, \qquad T=T_{in} \tag{5}$$

while pressure condition was imposed at the outlet section.

At the fluid-solid interface, no-slip boundary condition was considered for the fluid flow problem while continuity of temperature and heat flux was imposed for the thermal problem. The energy equation was simultaneously solved for enthalpy in solid and fluid regions. Consequently, the thermal condition at the fluid-solid interface was automatically met by the local energy balance. Other surfaces of the solid domain were considered to be adiabatic.
The local Nusselt number was evaluated as follows:

$$Nu = \frac{hD}{\lambda_f} = \frac{q_w D}{\lambda_f \left(T_w - T_b\right)} \tag{6}$$

where q_w is the wall heat flux, h is the convective heat transfer coefficient, D the tube internal diameter, T_w and T_b are the wall and fluid bulk temperature, respectively.
By considering the wall heat flux and the wall temperature averaged along the wall circumference, the circumferentially averaged Nusselt number was evaluated:

$$\overline{Nu} = \frac{\overline{q_w} D}{\lambda_f \left(\overline{T_w} - T_b\right)} \tag{7}$$

being $\overline{q_w}$ and $\overline{T_w}$ the circumferentially averaged wall heat flux and temperature, respectively.

The conjugate heat transfer problem (i.e. Eqs.(1) and (4)) together with its boundary conditions was investigated using the finite volume method. The simulations were carried out with the open-source CFD package OpenFOAM®, where the flow and energy equations were solved using unstructured and second-order accurate finite-volume schemes, within the framework of the SIMPLE (Semi-Implicit Method for Pressure-Linked Equations) algorithm [13]. For all governing equations, linear iterative solvers were used with an absolute tolerance equal to 1e-9. In particular, the pressure distribution within the fluid was solved using a Preconditioned Conjugate Gradient (PCG) solver, while an iterative solver that uses a smoother was used for determining both the velocity and temperature distributions in the fluid domain [14]. The solver with smoother was also used to solve the energy conservation equation in the solid region.

A limited linear or central convection scheme are used as divergence and gradient schemes, while a corrected linear scheme was used for the diffusive term of the governing equations. The computations were performed by means of an hybrid grid, consisting of hexahedral cells and created using the open-source software for mesh generation Gmsh [15].

4. Results

The model validation was carried out by considering the following operating conditions for which local experimental data were available in [11,12]: Pr=173 and Re=135.
To make sure that the solution was independent of the mesh resolution, several grids with different sizes were tested. Due to the interest of the present analysis in the hydrodynamically and thermally fully developed flow, for each considered grid, the local and the circumferentially averaged Nusselt number in the fully developed region were monitored.
To better evaluate the fluid-solid interface for all of the considered grids several thin layers were generated in both solid and fluid domains, as shown in Figure 3, where two representative outlet sections of the investigated grids are presented. It has to be pointed out that due to complexity of here considered geometry, several mesh parameters (i.e. the number of thin layers in both fluid and solid domains, the number of sections along the duct axis and the number of radial elements in the cross-section) can be varied to test the influence of the grid size on the numerical results. To check the

influence of the cells number on the fluid flow behaviour, all of the grid parameters were varied at the same time.

In Figure 4, the results of the mesh independence study are reported in terms of both circumferentially averaged and local Wall Shear Stress (WSS) for all of the here considered mesh sizes. In particular, in Figure 4a WSS averaged along the duct perimeter is depicted as a function of the dimensionless cell size (i.e. V^* was obtained by dividing the total cells volume by the minimum cells volume), while in Figure 4b local distribution of WSS is presented along the angular coordinate α, whose origin was taken at the extrados. It was observed that for a grid characterized by V^*=1.01e07 (i.e. about 4'400'000 cells) both the average and the local WSS could be assessed with a good accuracy.

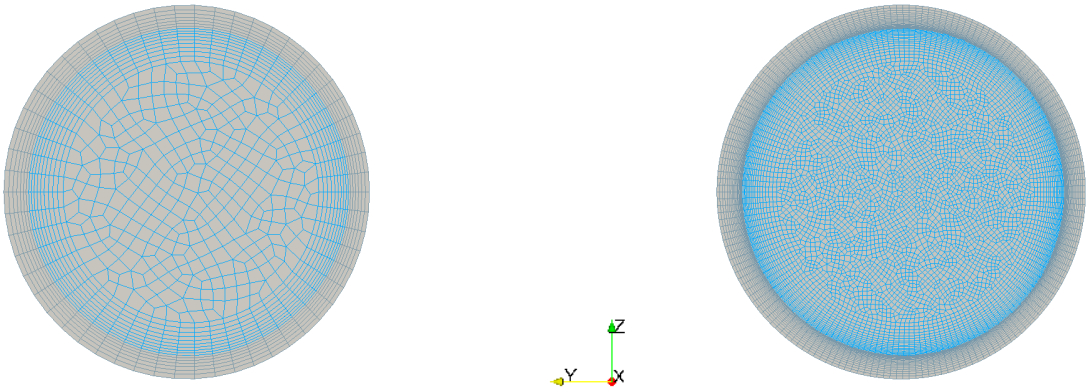

(a) (b)

Figure 3. Sketch of the investigated grids. Coarsest mesh (976'000 cells) (a) and finest mesh (12'500'000 cells) (b).

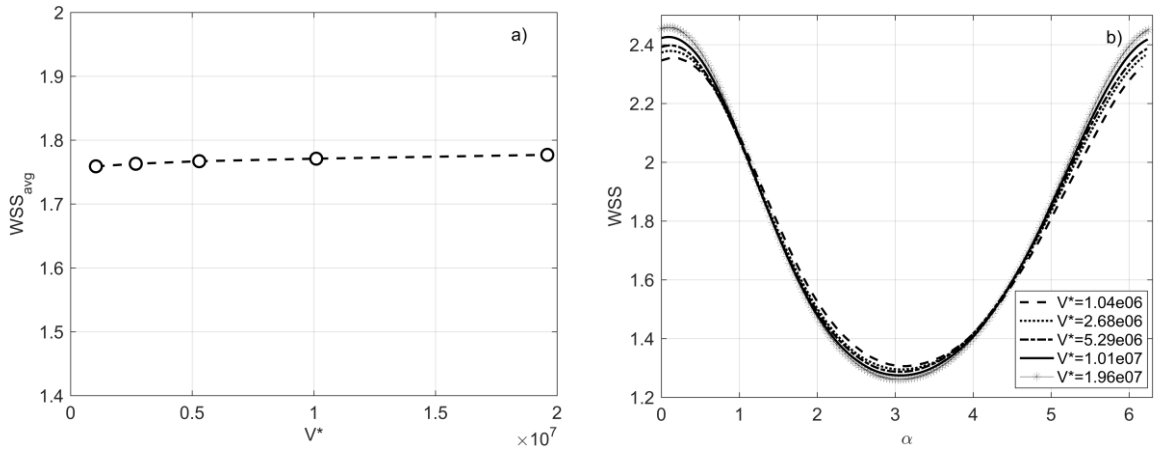

(a) (b)

Figure 4. Mesh convergence analysis. Average WSS (a) and local WSS (b).

Although the local fluid flow behaviour was correctly evaluated by using a mesh characterized by at least 4'385'000 cells, a further refinement was necessary to obtain a good accuracy in the evaluation of the fluid thermal behaviour, as shown in Figure 5, where the results of the grid convergence analysis are reported in terms of both circumferentially averaged and local Nusselt numbers. *Nu* averaged along the wall circumference as a function of the dimensionless cell size is depicted in Figure 5a. It can be noticed that with the grid refinement ranging from V^*=1.01e07 to V^*=1.96e07 the average Nusselt number only changes by less than 1.6%, which indicates that the results obtained by

adopting the grid with about 7'400'000 can be considered accurate. To assess the influence of the grid size on the evaluation of the local heat transfer phenomena, in Figure 5b the Nusselt number distribution along the angular coordinate is reported for all of the here considered mesh sizes. The data in Figure 5b confirm that the results obtained by adopting a mesh characterized by at least 7'400'000 cells (i.e. V^*=1.01e07) allow evaluating the local heat transfer with a good accuracy.

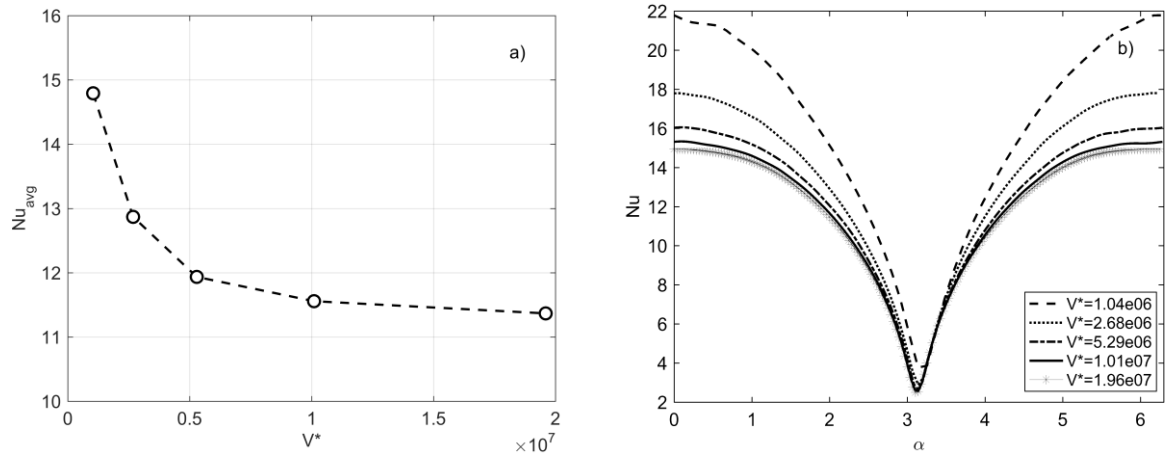

(a) (b)

Figure 5. Mesh convergence analysis. Circumferentially averaged Nusselt number (a) and local Nusselt number (b).

To validate the numerical model here adopted, the results obtained by using the finest mesh were compared to the experimental data presented in [11,12] in terms of local Nusselt number. In Figure 6 the numerical outcomes in terms of normalized Nusselt number distribution (i.e. $Nu_{ratio}=Nu/Nu_{max}$) along the angular coordinate are compared to experimental results. The comparison reveals that the numerical model enables to evaluate the local distribution of the heat transfer coefficient with a good accuracy, since the numerical results and experimental data are in good agreement. Moreover, in the same figure the results obtained by adopting the numerical model presented in the preliminary analysis [11] are presented. It can be observed that the present numerical model is more accurate in the evaluation of the local distribution of the Nusselt number ratio.

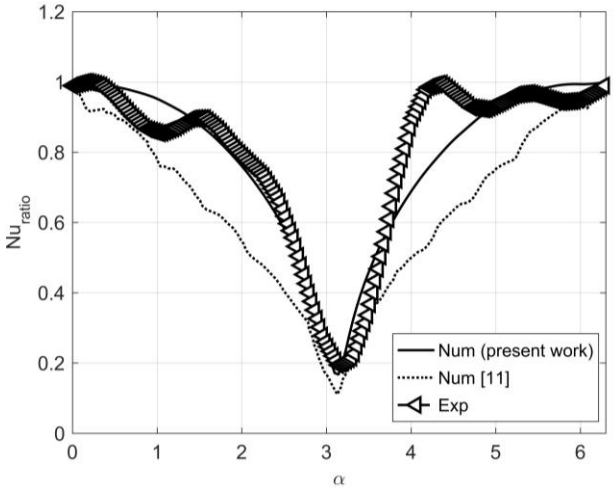

Figure 6. Comparison with experimental data and preliminary numerical results.

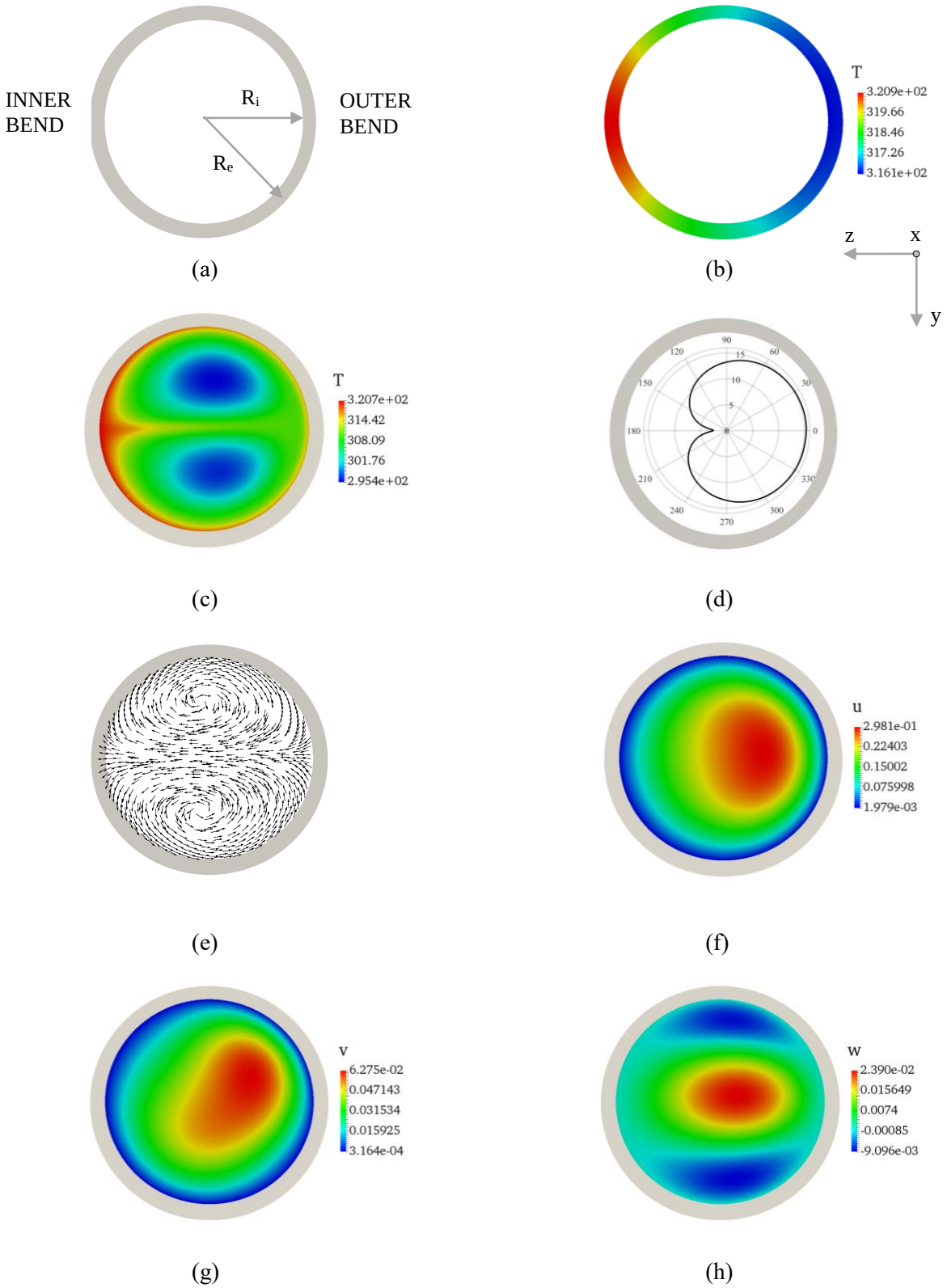

Figure 7. (a) Sketch of the outlet section; (b) wall temperature distribution [*K*]; (c) fluid temperature distribution [*K*]; (d) Nusselt number; (e) vortices; (f) *x*-component of the velocity vector [*m*/s]; (g) *y*-component of the velocity vector [*m*/*s*]; (h) *z*-component of the velocity vector [*m*/*s*].

Since the numerical model here adopted is robust and accurate, the numerical results can provide a good understanding of the physical phenomena, which take place in this kind of heat transfer device. In Figure 7 several representative results of the numerical runs are presented. The numerical outcomes clearly show that, as expected, the centrifugal force induces a secondary motion orthogonal to the main flow direction, which is characterized by the formation of a pair of vortices (i.e. the Dean vortices). These vortices presented in Figure 7e are responsible of the fluid temperature distribution shown in Figure 7c and of the Nusselt number distribution depicted in Figure 7d. In fact, as expected, the minimum of the convective heat transfer coefficient occurs at the extrados. To better evaluate the influence of the torsion induced by the coil pitch on the fluid velocity, the distributions of the velocity components u,v and w, which represent the components of the velocity vector along x, y and z, respectively, are also reported in Figure 7.

5. Conclusions

A numerical model able to capture the local heat transfer phenomena in laminar flow through helically coiled tubes was presented. To provide a good understanding of the local phenomena, the analysis was carried out by considering the conjugate heat transfer problem.

The flow and energy equations were solved by using the open-source CFD package OpenFOAM®, based on unstructured and second-order accurate finite-volume schemes, within the framework of the SIMPLE algorithm.

The experimental validation of the here adopted numerical model was carried out by comparing the experimental data obtained for ethylene glycol with the numerical results, in terms of both average and local distribution of the convective heat transfer coefficient. The good agreement between the predictions and the experimental evidences reveals that the numerical model offers a better insight in the heat transfer enhancement mechanism thus providing a useful tool to optimize the heat transfer devices.

Therefore, the here adopted numerical model will adopt to evaluate the influence of the main parameters that affect the fluid flow behavior, such as the Reynolds and Prandtl numbers, the Dean number, the thermal and geometrical properties of the wall (in order to evaluate the influence of the thermal boundary conditions as well). Moreover, the effect of the torsion induced by the coil pitch on the fluid flow behaviour will be investigated by considering several configurations.

Acknowledgments

The present work was partially supported by Regione Emilia Romagna, within POR-FESR 2014-2020, project HEGOS - nuove pompe di calore per l'Harvesting EnerGeticO in Smart buildings.
The numerical simulations were performed at CINECA High Performance Computing facilities, under the *HeTrE4TI* Project.

References

[1] Naphon P and Wongwises S 2004 A review of flow and heat transfer characteristics in curved tubes *Renew. Sust. Energ. Rev.* **10** 463–90
[2] Mori Y and Nakayama W 1967 Study on forced convective heat transfer in curved pipes (1st report, laminar region) *Int. J. Heat Mass Tran*. **8** 67–82
[3] Mori Y and Nakayama W 1967 Study on forced convective heat transfer in curved pipes (3rd report, theoretical analysis under the condition of uniform wall temperature and practical formulae) *Int. J. Heat Mass Tran*. **10** 681–95
[4] Mitsunobu A and Cheng KC 1971 Boundary vorticity method for laminar forced convection heat transfer in curved pipes *Int. J. Heat Mass Tran*. **14** 1659–75
[5] Patankar SV, Pratap VS and Spalding DB 1974 Prediction of laminar flow and heat transfer in helically coiled pipes *J. Fluid Mech.* **62** 539–51
[6] Kozo F and Aoyama Y 1988 Laminar heat transfer in a helically coiled tube *Int. J. Heat Mass*

Tran. **31** 387–96
[7] Zheng B, Lin CX and Ebadian MA 2000 Combined laminar forced convection and thermal radiation in a helical pipe *Int. J. Heat Mass Tran*. **43** 1067–78
[8] Yang G and Ebadian MA 1994 Perturbation solution for laminar convective heat transfer in a helix pipe *J. Heat Transf*. **116** 771–75
[9] Yang G, Dong ZF and Ebadian MA 1995 Laminar forced convection in a helicoidal pipe with finite pitch *Int. J. Heat Mass Tran*. **38** 853–62
[10] Ko TH 2006 Numerical investigation of laminar forced convection and entropy generation in a helical coil with constant wall heat flux *Numer. Heat Tr. A-Appl.* **49** 257–78
[11] Bozzoli F, Cattani L, Rainieri S and Zachár A 2015 Numerical and experimental study of local heat transfer enhancement in helically coiled pipes. Preliminary results *J. Phys. Conf. Ser.* **655** doi:10.1088/1742-6596/655/1/012047
[12] Bozzoli F, Rainieri S, Cattani L, and Pagliarini P 2013 Compound convective heat transfer enhancement in helically coiled wall corrugated tubes *Int. J. Heat Mass Tran*. **59** 353–62
[13] Ferziger, JH and Peric, M 2001 *Computational Methods for Fluid Dynamics* 3rd Ed. Springer: Berlin.
[14] Moukalled, F, Mangani, L and Darwish, M 2016 *The Finite Volume Method in Computational Fluid Dynamics* Springer International Publishing: Switzerland.
[15] Geuzaine C and Remacle JF 2013 A 3-D finite element mesh generator with built-in pre- and post-processing facilities *Int. J. Numer. Meth. Eng*. **79** 1309–31